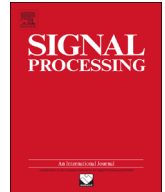




ELSEVIER

Contents lists available at SciVerse ScienceDirect

Signal Processing

journal homepage: www.elsevier.com/locate/sigpro

Robust estimation of highly-varying nonlinear instantaneous frequency of monocomponent signals using a lower-order complex-time distribution

Amir Omidvarnia^{a,*}, Ghasem Azemi^{a,b}, John M. O' Toole^c, Boualem Boashash^{a,d}

^a The University of Queensland, UQ Centre for Clinical Research, Herston QLD 4029, Brisbane, Australia

^b Department of Electrical Engineering, Razi University, Kermanshah, Iran

^c DeustoTech, University of Deusto, Bilbao, Spain

^d Qatar University, College of Engineering, Doha, Qatar

ARTICLE INFO

Article history:

Received 21 August 2012

Received in revised form

11 February 2013

Accepted 30 March 2013

Available online 18 April 2013

Keywords:

Time–frequency distribution

Instantaneous frequency

Estimation

Complex step differentiation

Nonstationarity

ABSTRACT

This paper proposes an approach for robust estimation of highly-varying nonlinear instantaneous frequency (IF) in monocomponent nonstationary signals. The proposed method is based on a lower order complex-time distribution (CTD), derived by using the idea of complex-time differentiation of the instantaneous phase. Unlike other existing TFDs in the same framework, the proposed TFD is an order-free distribution which alleviates the subtractive cancellation error in IF estimation. The approach is applied to highly nonstationary monocomponent signals. Performance of the numerical implementation is compared with three existing IF estimation methods using three simulated signals. Noise analysis is also performed to evaluate the robustness of the method in presence of additive noise at signal to noise ratio (SNR) varying from -10 dB to 20 dB. Results show that the proposed method outperforms the other methods at lower SNR and works reasonably well for the noiseless case.

© 2013 Elsevier B.V. All rights reserved.

1. Introduction

Dealing with nonstationary signals whose frequency content changes over time is a common problem in many research areas including biomedical signal processing [1], radar analysis [2], signal detection [3] and telecommunications [1,4]. The time-varying spectrum of nonstationary signals is discussed using the concept of instantaneous frequency (IF) [1,5,6]. A monocomponent nonstationary signal is defined as a signal whose time–frequency distribution (TFD) represents a single time-varying ridge in the time–frequency (T – F) domain. In contrast, a multi-component signal consists of two or more monocomponent signals, each of which has its own IF and instantaneous amplitude [7]. In practice, for the

vast majority of real signals, their corresponding TFDs may contain broadband noise as well as multiple spectral components [8]. Therefore, IF estimation of general nonstationary signals may require a pre-processing stage to decompose the signal into monocomponent signals, using methods such as time–frequency blind source separation [9,10], prior to applying monocomponent IF estimation techniques or it may require the design of specially adapted or reduced interferences realization for multicomponent signals [11].

A well-know approach for IF estimation is based on the extraction of the IF ridges in signal TFDs [5,6]. Several IF estimation methods belong to this class including model-based [12,13], Wigner–Ville distribution-based [1], L-Wigner distribution-based [14], polynomial Wigner–Ville distribution (PWVD)-based [15,16] and complex-time distribution-based [17–19] approaches. Among these, those based on complex-time distributions (CTDs) have been shown to be capable of estimating highly-varying nonlinear IFs [17,19]. The complex time argument was firstly introduced in [18] for CTDs where a

* Corresponding author. Tel.: +61 7 3346 5555; fax: +61 7 3346 5509.

E-mail addresses: a.omidvarnia@uq.edu.au, amir.omidvarnia@gmail.com (A. Omidvarnia).

derivative of function (here, instantaneous phase) was estimated based on its complex-argument Taylor expansion. Although the general form of CTDs has been well-established for all even orders in previous studies [11,17–20] (see also Eq. (7)), consideration of lower order IF approximation as a potential way of increasing robustness to noise has not received full attention in previous studies. This could be important, because higher order derivatives of a function are more vulnerable to noise compared to the lower orders. Therefore, the estimation of highly-varying IFs in nonstationary and noisy signals is still an open field of research [21]. This study proposes a lower order CTD, as a variant of the phase derivative estimation principle introduced in [18], derived using a robust approximation of the instantaneous phase (IP) derivative of the signal. The concept of complex-time argument has also been adapted for accurate numerical differentiation of a function, the so-called complex-step differentiation (CSD) [22]. The CSD is preferred over the standard finite difference since (i) it does not suffer from the *subtractive cancellation error*¹, (ii) it can be used for highly changing functions, (iii) it is applicable to general nonlinear functions, (iv) it is robust to noise, and (v) it retains a reasonable computational cost [23,24]. Therefore, it is a good choice for estimating the nonlinear and highly-varying IF laws in nonstationary and noisy signals. In this study, we show, using simulations, that the peak frequency of the proposed lower order CTD provides an accurate and robust estimate of the highly-varying IFs. We also show that the proposed IF estimation method is comparable with and in some cases, superior to existing IF estimators specifically designed for highly nonstationary signals [16,19].

The organization of this paper is as follows. Section 2 reviews the theoretical background associated with the TFDs designed for representing highly nonstationary signals along with the concept of complex-time argument differentiation. Section 3 details the proposed lower order CTD and its associated IF estimation procedure as well as the numerical implementation. In section 4, the performance of the proposed method is evaluated and compared with four existing methods using three simulated signals. Noise analysis is also performed using Monte-Carlo simulations to assess the robustness of the methods in the presence of noise. Section 5 concludes the paper. The relevant steps for the mathematical proofs related to the properties of the proposed distribution are given in the [Appendix](#).

2. TFDs with complex-time argument differentiation

Let $z(t)$ be the *normalized analytic associate* [1] of a real-valued monocomponent signal $x(t)$, given by

$$z(t) = e^{j\varphi(t)} \quad (1)$$

where $\varphi(t)$ denotes the IP of the signal. The IF law of $z(t)$ is defined as [1]

$$f_i(t) = \frac{1}{2\pi} \frac{d\varphi(t)}{dt}. \quad (2)$$

Ideally, a TFD of $z(t)$ should exhibit a unit delta function along the IF as [1]:

$$\rho_z(t, f) = \delta(f - f_i(t)) \quad (3)$$

where $\delta(\cdot)$ denotes the Dirac delta function. By taking the inverse Fourier transform with respect to f from Eq. (3), the signal kernel (also called *instantaneous autocorrelation function—IAF*) of the signal is obtained as [1]

$$K_z(t, \tau) = \mathcal{F}_{\tau \rightarrow f}^{-1} \{\rho_z(t, f)\} = e^{j2\pi f_i(t)\tau} = e^{j\varphi'(t)\tau} \quad (4)$$

where $\mathcal{F}_{\tau \rightarrow f}^{-1}$ denotes the inverse Fourier transform from the frequency domain to the lag domain. In the classical definition of the WVD, the differentiation term $\varphi'(t)$ is approximated by

$$\varphi'(t) \approx \frac{\varphi(t + \frac{\tau}{2}) - \varphi(t - \frac{\tau}{2})}{\tau} \quad (5)$$

which leads to the well-known form of this distribution [1] as

$$\text{WVD}_z(t, f) = \mathcal{F}_{\tau \rightarrow f} \{K_z(t, \tau)\} = \int_{-\infty}^{\infty} z\left(t + \frac{\tau}{2}\right) z^*\left(t - \frac{\tau}{2}\right) e^{-j2\pi f\tau} d\tau. \quad (6)$$

For the polynomial IFs with phase order of 2 or higher, the WVD introduces pseudo-information in the T - F domain in the form of inner cross-terms [15,25]. In particular, these cross-terms become severely problematic when the IF is nonlinear and highly-varying over time. Complex-time argument TFDs and PWVDs have been suggested to improve the estimation of highly-varying and/or nonlinear IFs by employing the higher order derivatives of the IP in the time-lag domain. The general form of an N -order TFD with a complex-time argument is defined as [19]

$$\text{CTD}_z^{(N)}(t, f) = \int_{-\infty}^{\infty} P(\theta) SM(t, f + \theta) C(t, f - \theta) d\theta \quad (7)$$

where N is an even integer, $P(\theta)$ is a smoothing window and $SM(t, f)$ is defined as

$$SM(t, f) = \int_{-\infty}^{\infty} P(\theta) STFT(t, f + \theta) STFT^*(t, f - \theta) d\theta \quad (8)$$

where $STFT$ stands for the short time Fourier transform. $C(t, f)$ is given by

$$C(t, f) = \int_{-\infty}^{\infty} P(\theta) C_r(t, f + \theta) C_i(t, f - \theta) d\theta \quad (9)$$

where $C_r(t, f)$ and $C_i(t, f)$ are defined based on the N complex roots $\omega_{N,p}$ on the unit circle ($\omega_{N,p} = e^{j(2\pi p/N)}$). Throughout this paper, we use the acronym *CTD* to refer to this family of TFDs. To improve the concentration of energy around the IF law (decreasing the spread factor²), L -form of the CTDs was introduced in [19,26] as:

$$\text{LCTD}_z^{(N,L)}(t, f) = \int_{-\infty}^{\infty} \prod_{l=1}^{N/2} z\left(t + \frac{\tau}{LN(a_l + jb_l)}\right)^{\pm L(a_l + jb_l)} e^{-j2\pi f\tau} d\tau. \quad (10)$$

¹ In floating-point computations, the subtraction of nearly equal floating-point numbers may lead to the loss of significant digits. This error is referred to as the subtractive cancellation error.

² Spread factor in the TFDs is a time-lag function which determines the distribution spread around the instantaneous frequency [18].

Table 1
Definitions of the 4th order CTD and the 4th order PWVD.

TFD	Definition
4 th order CTD [19]	$CTD_z^{(4)}(t,f) = \int_{-\infty}^{\infty} z(t + \frac{\tau}{4})z^*(t - \frac{\tau}{4})z'(t + j\frac{\tau}{4})z'(t - j\frac{\tau}{4})e^{-j2\pi f\tau}d\tau$
4 th order PWVD [16]	$PWVD_z^{(4)}(t,f) = \int_{-\infty}^{\infty} (z(t + \frac{\tau}{4}))^2(z^*(t - \frac{\tau}{4}))^2e^{-j2\pi f\tau}d\tau$

The definition of the polynomial WVD (PWVD) with order N is given by [16]

$$PWVD_z^{(N)}(t,f) = \int_{-\infty}^{\infty} \prod_{l=1}^{N/2} z(t + h_l\tau)z^*(t + h_{-l}\tau)e^{-j2\pi f\tau}d\tau \quad (11)$$

where N is an even integer and $h_l (l = 1, \dots, N/2)$ are constant real coefficients. For example, Table 1 presents the mathematical descriptions of $CTD_z^{(4)}(t,f)$ and 4th $PWVD_z^{(4)}(t,f)$, while the definition of $CTD_z^{(6)}(t,f)$ can be found in [19].

The indicated TFDs go beyond the quadratic form of the WVD to better concentrate the TF energy around the true IF. This, however, means higher computational cost and more vulnerability to noise. In this paper, we propose an IF estimation method which uses a TFD representing the second order of the phase derivative for maximum robustness and minimum computational cost, while preserving the ability of tracking fast-changing IFs in monocomponent nonstationary signals. The original WVD, the 4th order L-form CTD ($LCTD_z^{(4,3)}(t,f)$, $L = 3$) and the 6th order L-form CTD ($LCTD_z^{(6,3)}(t,f)$, $L = 3$) are employed in order to evaluate the performance of the proposed approach using simulated monocomponent signals.

Theoretically, a higher order differentiation of the IP in the CTDs and PWVDs yields more accurate estimation of the highly-varying IFs (smaller spread factor [18]). But, it is at the expense of higher computational complexity and vulnerability to noise. The proposed approach provides a robust estimate of the derivative of the IP function using a lower order CTD as a variant of the CTDs family [18]. We show that the method is comparable, and in some cases, more efficient than the IF estimators based on LCTDs [17,19] in noisy and highly nonstationary environments. To evaluate the methods, we have adapted the general form of the simulated nonstationary signals in Virtual Instrument toolbox [19].

3. Design of a complex-time distribution for IF estimation

This section describes the methodology for designing the lower order CTD and lists its properties, while the mathematical proofs can be found in the Appendix. We also discuss the numerical implementation aspects and other related practical issues.

3.1. A modified form of the WVD: definition and properties

The complex-time argument differentiation introduced in [18] is based on a Taylor series expansion of a real function $\varphi(t)$ about a real point t using a purely imaginary

step $j\tau$ as follows:

$$\varphi(t + j\tau) = \varphi(t) + j\tau\varphi'(t) - \frac{\tau^2\varphi''(t)}{2!} - j\frac{\tau^3\varphi'''(t)}{3!} + \dots \quad (12)$$

Taking the imaginary parts from both sides of Eq. (12) and dividing them by τ will result in an approximation for $\varphi'(t)$, referred to as complex-step differentiation (CSD) given by [22]:

$$\varphi'(t) \approx \frac{Im\{\varphi(t + j\tau)\}}{\tau} \quad (13)$$

The general form of the IAF in Eq. (4) can be written based on the CSD formulation presented in Eq. (13) yielding a new form for the signal kernel $K_z(t, \tau)$. By substituting Eq. (13) into Eq. (4), we obtain:

$$e^{j\varphi'(t)\tau} \approx e^{Im\{\varphi(t + j\tau)\}} \quad (14)$$

where τ is small. According to Eq. (1), $z(t + j\tau) = e^{j\varphi(t + j\tau)}$ and therefore, the signal kernel given by Eq. (14) can be written as

$$K_z(t, \tau) = e^{Im\{\varphi(t + j\tau)\}} = |z(t + j\tau)|^{-j} \quad (15)$$

where $|\cdot|$ represents the absolute value operator. The proposed CTD is then defined as the Fourier transform of $K_z(t, \tau)$ with respect to τ :

$$W_z^{CL}(t,f) = \mathcal{F}_{\tau \rightarrow f}\{K_z(t, \tau)\} = \int_{-\infty}^{\infty} |z(t + j\tau)|^{-j} e^{-j2\pi f\tau}d\tau \quad (16)$$

The $W_z^{CL}(t,f)$ given in Eq. (16) can be written as the general form of an energy distribution concentrated along its IF:

$$W_z^{CL}(t,f) = \int_{-\infty}^{\infty} e^{j\tau\varphi'(t) - j\frac{\tau^3}{3!}\varphi'''(t) + j\frac{\tau^5}{5!}\varphi^{(5)}(t) + \dots} e^{-j2\pi f\tau}d\tau \\ = 2\pi\delta(2\pi f - \varphi'(t)) * \mathcal{F}_{\tau \rightarrow f}\{e^{jQ(t,\tau)}\} \quad (17)$$

where $Q(t, \tau)$ is the spread factor of $W_z^{CL}(t,f)$ given by

$$Q(t, \tau) = -\frac{\tau^3}{3!}\varphi'''(t) + \frac{\tau^5}{5!}\varphi^{(5)}(t) + \dots \quad (18)$$

Performing the same calculation for the WVD, we get the spread factor as

$$Q_{WVD}(t, \tau) = \frac{\tau^3}{2^2 3!}\varphi'''(t) + \frac{\tau^5}{2^4 5!}\varphi^{(5)}(t) + \dots \quad (19)$$

Compared to the CTDs and PWVDs with $N > 2$, similar to the WVD, $W_z^{CL}(t,f)$ preserves the first order of the phase derivative only which in turn leads to a higher truncation error³ (order $O(\tau^2)$) reflected in its spread factor $Q(t, \tau)$ (Eq. (18)). However, there is another source of error in using finite difference approximations in the CTDs and PWVDs, the so-called subtractive cancellation error [22,27]. As an

³ Truncation error is generated when an infinite sum is truncated and approximated by a finite sum.

example, the cause of this error is explained by the expressions for the $CTD_z^{(4)}(t, f)$ in Table 1. The signal kernel of $CTD_z^{(4)}(t, f)$ can be obtained by the approximation of $\varphi'(t)$ to the fifth order using the Taylor series of $\varphi(t)$ with complex arguments:

$$\varphi'(t) \approx \frac{1}{j\tau} \left[\varphi\left(t + j\frac{\tau}{4}\right) - \varphi\left(t - j\frac{\tau}{4}\right) + j\varphi\left(t + \frac{\tau}{4}\right) - j\varphi\left(t - \frac{\tau}{4}\right) \right]. \quad (20)$$

This leads to the definition of the signal kernel $K_z(t, \tau)$ for the $CTD_z^{(4)}(t, f)$ as follows:

$$K_z(t, \tau) = e^{j\varphi'(t)\tau} \approx e^{j\varphi\left(t + j\frac{\tau}{4}\right) - \varphi\left(t - j\frac{\tau}{4}\right) + j\varphi\left(t + \frac{\tau}{4}\right) - j\varphi\left(t - \frac{\tau}{4}\right)} \quad (21)$$

$$\approx z^{-j}\left(t + j\frac{\tau}{4}\right) z^j\left(t - j\frac{\tau}{4}\right) z\left(t + \frac{\tau}{4}\right) z^*\left(t - \frac{\tau}{4}\right) \quad (22)$$

Eq. (22) clearly shows that the signal kernel is affected by the subtractive cancellation error between close values of $\varphi\left(t + (\tau/4)\right)$ and $\varphi\left(t - (\tau/4)\right)$ as well as $\varphi\left(t + j(\tau/4)\right)$ and $\varphi\left(t - j(\tau/4)\right)$. The advantage of adapting Eq. (13) as the phase derivative is that in most cases, the truncation error can be alleviated by selecting small τ , without the risk of increasing the subtractive cancellation error [22,27]. This property makes the CSD approximation tools suitable for sensitivity analysis, as they reflect issues of simple numerical implementation, accuracy and robustness together [24]. The lower order IF estimation method does not suffer from the subtractive cancellation error. This makes the method robust to noise, whilst maintaining a reasonable computational cost. However, one should bear in mind that choosing a too narrow lag window is not generally recommended for computing T - F representations of signals with fast varying IFs, as it lowers the frequency concentration and may introduce bias to the estimation. The main difference between Eq. (13) and the phase derivative used in the WVD ($\varphi'(t)\tau = \varphi\left(t + \tau/2\right) - \varphi\left(t - \tau/2\right)$) is that the subtractive cancellation error can be avoided in the former one.

The complex-time analytic associate $z(t + j\tau)$ needed for computing CTDs can be obtained using the idea introduced in [18,19]. Assuming that $Z(f)$ is the Fourier transform of the analytic associate $z(t)$, we have:

$$z(t + j\tau) = \int_{-\infty}^{\infty} Z(f) e^{-2\pi f \tau} e^{j2\pi f t} df. \quad (23)$$

and therefore:

$$z(t + j\tau) = \mathcal{F}_{t \rightarrow f}^{-1} \left\{ \mathcal{F}_{t \rightarrow f} \{z(t)\} e^{-2\pi f \tau} \right\}. \quad (24)$$

It can be shown that the modified form of the WVD in Eq. (16) satisfies most desired properties of a TFD as listed below, for the signal $z(t)$ with the general form of Eq. (1)

P1. Realness: $W_z^{CL}(t, f)$ is always real at any time and frequency.

P2. Time shift: if $W_z^{CL}(t, f)$ is the TFD of the signal $z(t)$, then $W_z^{CL}(t-T, f)$ is the TFD of the signal $z(t-T)$.

P3. Frequency shift: if $W_z^{CL}(t, f)$ is the TFD of the signal $z(t)$, then $W_z^{CL}(t, f-f_0)$ is the TFD of the signal $z(t)e^{j2\pi f_0 t}$.

P4. Time-frequency scaling: if $z_1(t) = z(at)$, then $W_{z_1}^{CL}(t, f) = 1/|a| W_z^{CL}(at, f/a)$.

P5. Time marginal: integration of $W_z^{CL}(t, f)$ over the

frequency axis (time marginal distribution) results in:

$$\int_{-\infty}^{\infty} W_z^{CL}(t, f) df = |z(t)|^2, \quad z(t) \neq 0. \quad (25)$$

P6. Instantaneous frequency: the first order moment of $W_z^{CL}(t, f)$ with respect to frequency yields the IF of the signal $z(t)$:

$$\frac{\int_{-\infty}^{\infty} f W_z^{CL}(t, f) df}{\int_{-\infty}^{\infty} W_z^{CL}(t, f) df} = \frac{1}{2\pi} \frac{d\{\arg(z(t))\}}{dt} = \frac{1}{2\pi} \frac{d\varphi(t)}{dt}. \quad (26)$$

P7. Modulation invariance: if $z(t) = z_1(t)z_2(t)$, then:

$$W_z^{CL}(t, f) = W_{z_1}^{CL}(t, f) *_{(f)} W_{z_2}^{CL}(t, f). \quad (27)$$

The mathematical proofs of the above properties can be found in the Appendix.

3.2. A lower order CTD based on the modified WVD

The dichotomic impact of the lag window length in the proposed lower order CTD may impose unwanted fluctuations in the T - F domain which can be attenuated using e.g. Gaussian filtering. The final representation of the proposed lower order CTD is therefore given by

$$\rho_z^{CL}(t, f) = \mathcal{F}_{\tau \rightarrow f} \{g_2(\tau) \{K_z(t, \tau) *_{(t, \tau)} g_1(t, \tau)\}\} \quad (28)$$

where $g_1(t, \tau)$ is a local time-lag Gaussian filter and $g_2(\tau)$ is a Gaussian lag-window. Note it is also necessary to apply similar filtering on the whole family of CTDs in general (for example, see Eqs. (7)–(9)). In order to extract the IF law of monocomponent nonstationary signals, the ridge (peak frequency at each time sample) of the TFDs can be used (see Table 3).

3.3. Numerical implementation of the lower order CTD

The lower order CTD can be described in the discrete-time domain as

$$W_z^{CL}[n, k] = \mathcal{F}_{m \rightarrow k} \{K_z[n, m]\} \quad (29)$$

where $K_z[n, m] = |z[n + jm]|^{-j}$ and $\mathcal{F}_{m \rightarrow k}$ denotes the discrete Fourier transform from the lag domain to the frequency domain. The discrete-time form of the complex-time analytic associate $z[n + jm]$ is obtained using [18]:

$$z[n + jm] = \frac{1}{N} \sum_{k=1}^{N_{\text{sig}}} Z[k] e^{-\frac{2\pi m k}{N_{\text{sig}}}} e^{j\frac{2\pi n k}{N_{\text{sig}}}} \quad (30)$$

where $Z[k] = \mathcal{F}\{z[n]\}$ and N_{sig} is the length of $z[n]$ in samples. In practice, direct usage of Eq. (30) for the final-length digital signals does not lead to satisfactory results [28]. In fact, a finite-duration signal can be considered as the multiplication of an infinite signal with a rectangular window in the time domain. Such temporal multiplication creates new smearing components in the frequency domain (also referred to as *spectral leakage*) spreading throughout the whole time-lag plane (see also Eqs. (23) and (24)). In addition, Eq. (30)

requires sample points in the discrete version of $z(t + j\tau)$ which are not available in $z[n]$ and are only approximated by interpolation. It results in another source of approximation error in the numerical implementation of $z[n + jm]$. Therefore, although the continuous forms of the CTDs are real-valued for the general signal type of Eq. (1), the numerical forms may not be necessarily real-valued. In order to avoid the cross-terms arising due to the aforementioned problems, time-lag filtering is included to the numerical implementation of all CTDs (see also Eqs. (7)–(9)). For the proposed TFD, a local time-lag Gaussian filter $g_1[n, m]$ with the size $[h, h]$, $h \in \mathbb{N}$ and the standard deviation σ_1 is convolved to $K_z[n, m]$. Another Gaussian lag-window $g_2[m]$ with the standard deviation σ_2 also suppresses the remaining fluctuations in the frequency domain. The final realization of the lower order TFD $\rho_z^{CL}[n, k]$ is expressed as

$$\begin{aligned} \rho_z^{CL}[n, k] &= \mathcal{F}_{m \rightarrow k} \left\{ g_2[m] (K_z[n, m] \underset{(m,n)}{**} g_1[n, m]) \right\} \\ &= \sum_{m=1}^{N_{sig}} \sum_{p=-h/2}^{h/2} \sum_{q=-h/2}^{h/2} g_2[m] g_1[p, q] K_z[n-p, m-q] e^{j\frac{2\pi m k}{N_{sig}}} \end{aligned} \quad (31)$$

For the proposed lower order CTD, the standard deviations σ_1 and σ_2 were set to 1 and 10, respectively. Note that g_1 and g_2 do not need to be Gaussian necessarily. See e.g. the windows g_1 and g_2 used in [29]. Gaussian filtering ($\sigma = 7$) was also performed for both 4th and 6th order CTDs [19]. Also, the lag window length for the WVD was set to $N_{sig} - 1$. MATLAB implementations of the CTDs were provided from Virtual Instrument toolbox [19] and the WVD implementation was obtained from the TFSA toolbox [30].

3.4. IF estimation

According to the property **P6** of $W_z^{CL}(t, f)$, the first order moment of $\rho_z^{CL}[n, k]$ with respect to frequency provides an estimate of the IF law of the monocomponent nonstationary signals. Also, by definition, the dominant knife-

edge ridge of $\rho_z^{CL}[n, k]$ (associated with the spectral maxima of the TFD along the time axis) leads to an estimate of the IF [1]. The discrete-time linear moment IF estimator is defined as [1]

$$\hat{f}_i[n] = \frac{F_s}{2N_{sig}} \frac{\sum_{k=0}^{N_{sig}-1} k \rho_z^{CL}[n, k]}{\sum_{k=0}^{N_{sig}-1} \rho_z^{CL}[n, k]} \quad 1 < n < N_{sig} \quad (32)$$

whereas the peak frequency is given by [1]

$$\hat{f}_i[n] = \frac{1}{2N_{sig}} \left\{ \arg \left\{ \max_k \rho_z^{CL}[n, k] \right\} - \frac{N_{sig}}{2} \right\} \quad 1 < n < N_{sig} \quad (33)$$

where $\rho_z^{CL}[n, k]$ is of the size $N_{sig} \times N_{sig}$. Note that the subscript i is not an index number, but it stands for ‘instantaneous’. The definition of the peak frequency will be used in this study to extract the IF laws of three nonstationary signals in the absence or presence of noise to evaluate the performance of different TFDs.

4. Performance evaluation and discussion

In this section, the proposed IF estimation method and four other existing methods are applied on selected simulated signals. The normalized root mean squared error (NRMSE) cost function is used to compare the performance of the different estimators.

Table 2

List of the IP laws used for generating the simulated signals.

Signal	$\varphi(t)$ IP law ()
A	$3\cos[\pi n] + 2\cos[2\pi n] - 3\cos[3\pi n]$
B	$3\cos[2\pi n] + 0.75\cos[6\pi n] + 0.75\cos[10\pi n]$
C	$3\cos[\pi n] + 0.5\cos[15\pi n] + 0.5\cos[12\pi n]$

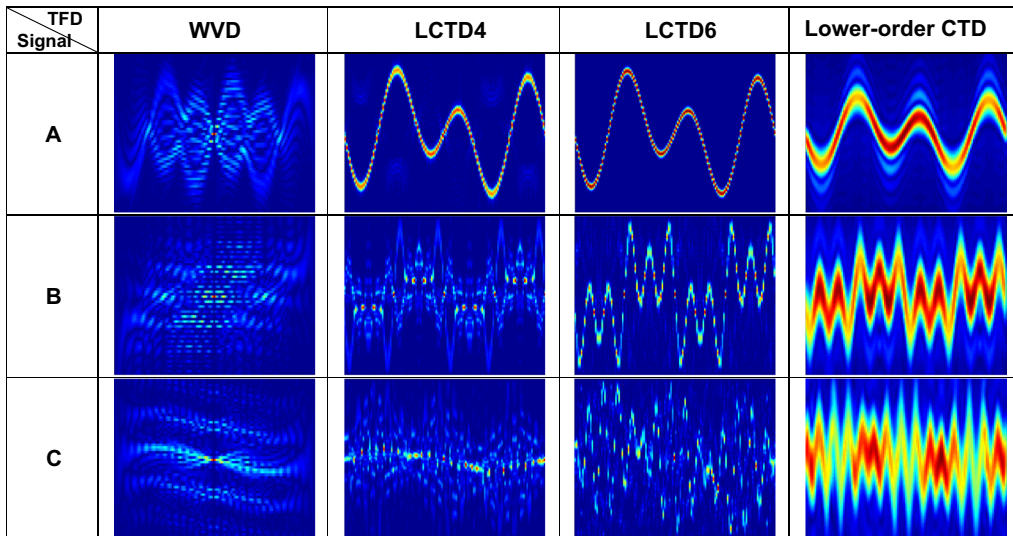


Fig. 1. Absolute values of the TFDs extracted from 2 s segments of the simulated signals introduced in Table 2.

4.1. Performance measure

In order to evaluate the performance of the proposed IF estimation method, 128-sample segments of three mono-component nonstationary signals with IP laws listed in Table 2 were simulated ($F_s = 64$ Hz). The general form of the simulated signals was taken from the Virtual Instrument toolbox [19], designed for T-F analysis of signals with highly nonstationary IP laws. Then, the performance of the IF estimators based on the peak of WVD, 4th order LCTD (LCTD4) and 6th order LCTD (LCTD6) [19] were compared against the proposed method. The comparison results were quantified with the NRMSE of the IF estimation over a large number of Monte-Carlo simulations defined as:

$$NRMSE = 1 - \frac{1}{N_{MC}} \sum_{r=1}^{N_{MC}} \frac{\|\mathbf{f}_i - \hat{\mathbf{f}}_i^r\|}{\|\mathbf{f}_i - \text{mean}(\hat{\mathbf{f}}_i^r)\|} \quad (34)$$

where $\|\cdot\|$ represents the Euclidian norm, $\hat{\mathbf{f}}_i^r$ is the IF estimate at the run r and N_{MC} is number of Monte-Carlo runs (here, $N_{MC} = 100$) (note that, as mentioned before, the subscript i stands for ‘instantaneous’). The NRMSE mea-

sure ranges between $-\infty$ (bad fit) to 1 (perfect fit) between the reference IF function (\mathbf{f}_i) and its estimated version ($\hat{\mathbf{f}}_i$).

4.2. Simulation results

The IP of the simulated signals are listed in Table 2. Fig. 1 illustrates the TFDs extracted from the simulated signals of length 128 sample ($F_s = 64$ Hz), detailed in Table 2.

In Fig. 1, each row corresponds to one of the three simulated signals and each column represents the outputs of a certain TFD for the simulated signals.

Fig. 2(a)–(c) illustrates the estimated IF laws of the simulated signals in Table 2 using the frequency peak IF estimator. Each panel depicts the original IF law as well as its estimated versions using LCTD of order 4, LCTD of order 6, the WVD and the lower order CTD.

Table 3 summarizes the performance evaluation results using the NRMSE measure for the above signals in the absence of noise.

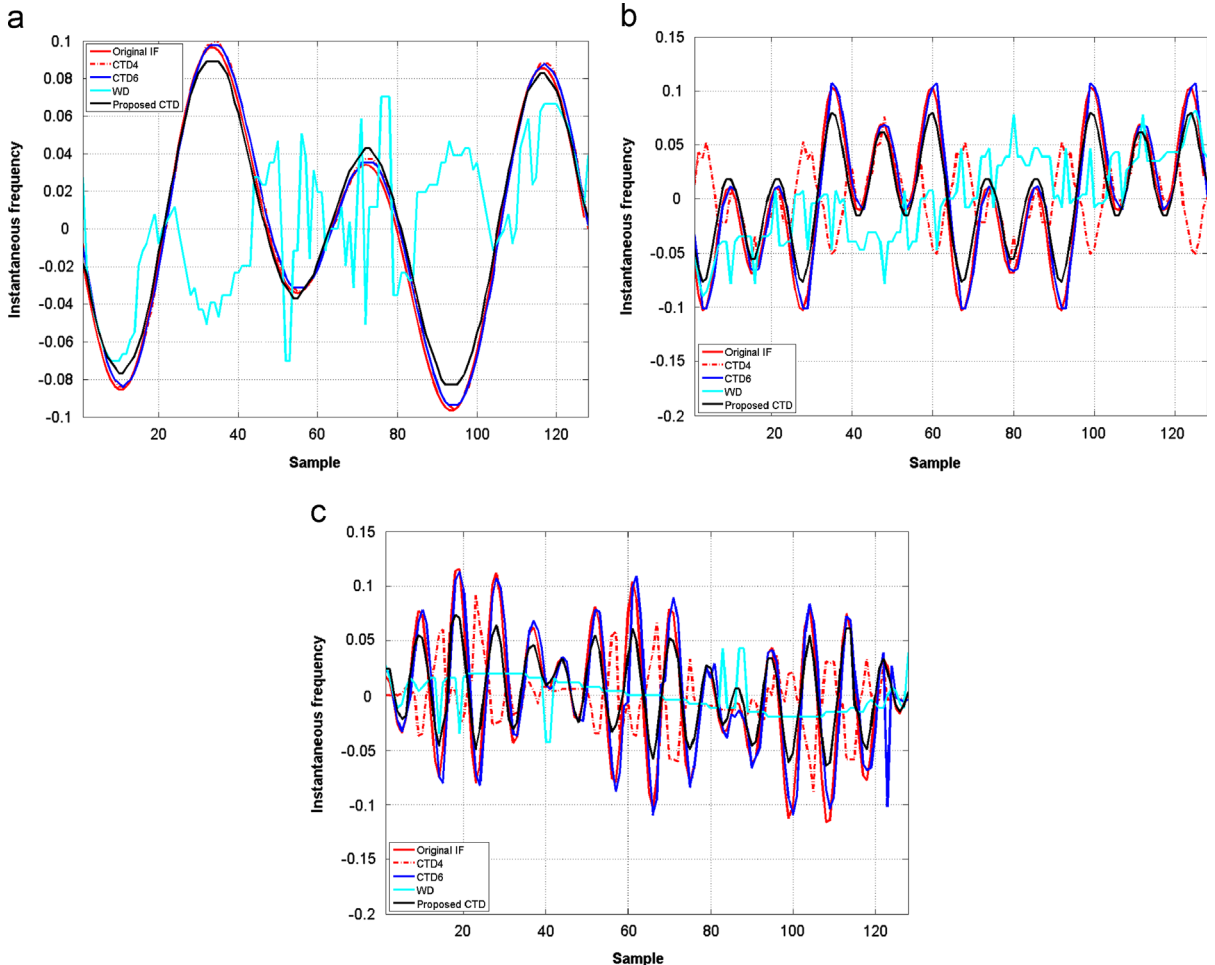


Fig. 2. Original IF laws and the estimated IF laws for the simulated signals in Table 2 using the peak frequency estimator: (a) signal A, (b) signal B and (c) signal C.

4.3. Noise analysis

Robustness of the IF estimators in the presence of noise was assessed using Monte-Carlo simulations with 100 iterations. In each iteration, white Gaussian noise processes with different signal to noise ratio (SNR) covering the interval -10 to 20 dB were added to the simulated signals described in Table 2. The IF estimation methods were applied to the noisy signals and the average NRMSE measure was calculated.

Fig. 3 illustrates the performance of the methods for the three selected simulated signals.

4.4. Discussion

The previous results illustrated the usefulness of robust estimation of highly-varying nonlinear IF in monocomponent signals under noisy circumstances using the proposed lower-order CTD. The performance of the method evaluated using the NRMSE cost function for three simulated signals indicates that in the absence of noise, the variance of the IF estimate using the lower order CTD is higher than LCTD6 (Fig. 2). This relates to the fact that the spread factor of the lower order

CTD (Eq. (18)) preserves lower orders of the exponential lag terms in the Taylor series expansion of the IP function. Also, as the dynamics of the signals gets faster (the nonlinear IF changes more rapidly), the bias of the estimate increases compared with LCTD6 (see Fig. 2). This is also reflected in the decreasing trend in the NRMSE measures of the lower order CTD in Table 3. LCTD4 performs well for nonlinear IFs with moderate variation, but it degrades drastically when the IF law changes more rapidly (notice the drop in the NRMSE measure of LCTD4 from 0.92 for signal A to -0.23 and -0.35 for signal B and signal C, respectively). As expected, the WVD

Table 3

NRMSE cost (between the estimated IFs and original IFs using the peak frequency estimator).

Signal	Method			
	WVD	LCTD4	LCTD6	Lower order CTD
Signal A	-0.13	0.92	0.92	0.88
Signal B	-0.08	-0.23	0.80	0.71
Signal C	0.00	-0.35	0.58	0.57

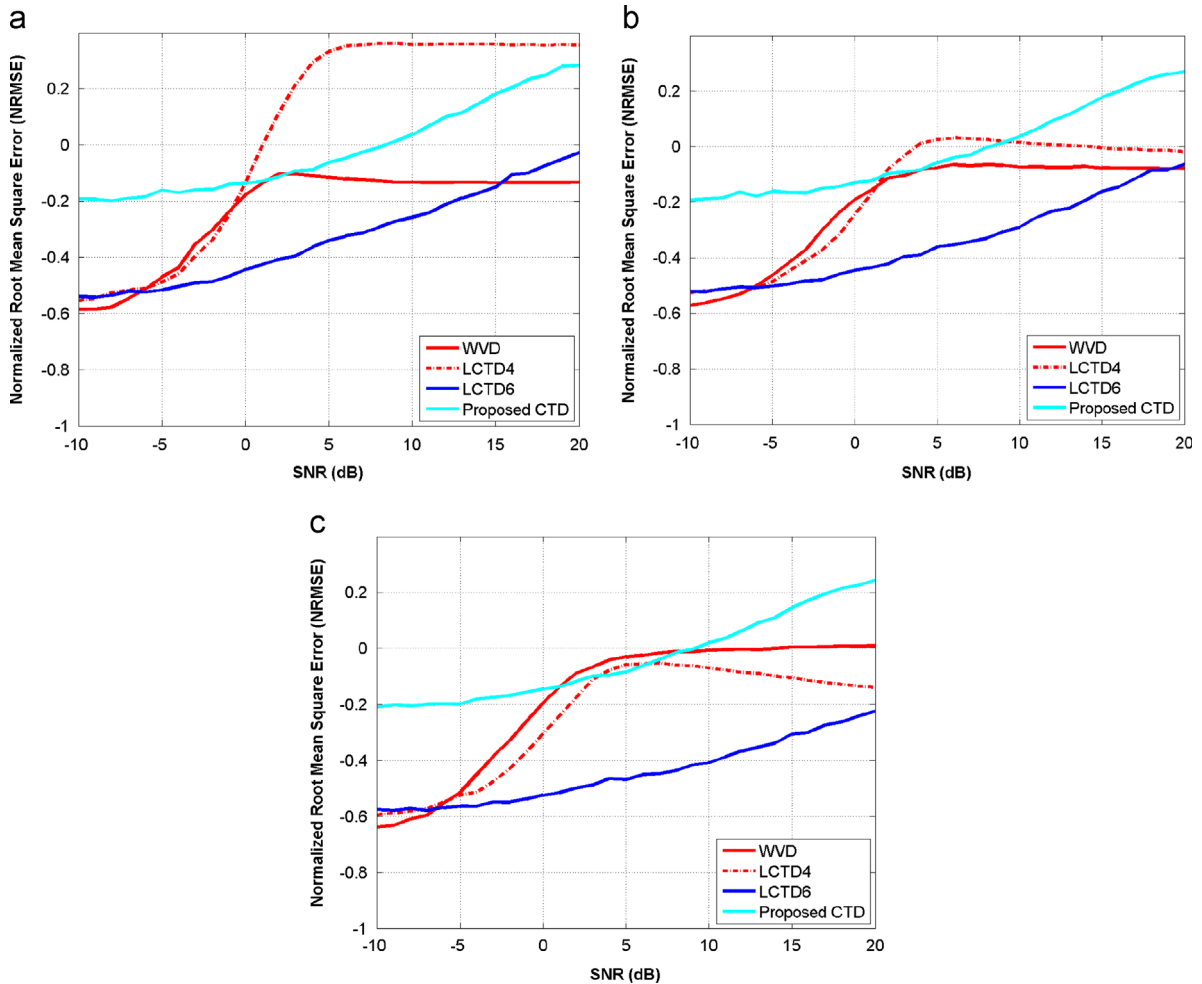


Fig. 3. NRMSE measure for different IF estimators applied on signal A (a), signal B (b) and signal C (c).

shows the lowest performance among all TFDs of this study in the absence of noise.

In the presence of noise, LCTD4 outperforms LCTD6 for all three simulated signals implying that an increase in the order of LCTDs may have negative impact on robustness to noise. At low levels of noise (5 to 20 dB), LCTD4 shows the highest performance among other TFDs for signal **A** (Fig. 3a), while it degrades for signal **B** and signal **C** with more rapid-changing IFs. A mild but consistent decreasing trend in the performance of LCTD4 on signal **B** and signal **C** within 5–20 dB SNR interval suggests that the highly-changing behavior in the less noisy signals is more destructive compared with heavily noisy signals, as the performance may be dominated by the speed of variation in the IF law rather than the noise level. Although LCTD6 represents less error estimate than the proposed lower-order CTD on noiseless signals (Table 3), it decays considerably in noisy conditions (even low levels) in contrast to the lower order CTD (see Fig. 3). In the highest changing situation (i.e., signal **C**), LCTD4 and LCTD6 are even less efficient than the classical WVD re-emphasizing the dichotomic role of the Taylor series order on the LCTD-based IF estimation methods. It suggests that preserving the higher order derivatives in IF estimation methods may make the estimator more vulnerable to noise. One, however, should note that such robustness is obtained at the expense of increase in the bias and spread of the IF estimates.

Lower order CTD outperforms the other distributions during highly noisy conditions (-10 to 5 dB—see Fig. 3) by showing an increasingly robust behavior on all three simulated signals. Performance of the WVD and LCTD4 is more or less the same as reflected in their NRMSE measures starting almost from -0.6 and reaching roughly to -0.2. LCTD6 shows the weakest performance amongst the other TFDs in this SNR interval, while its efficiency recovers monotonically by reducing the noise level. All in all, the lower-order CTD combined with the IF peak detector maintains its performance for highly noisy environments (-10 to 5 dB) in terms of the NRMSE measure, while the other CTD-based estimators lose their efficiency significantly (see Fig. 3).

This study deals only with the case of nonstationary monocomponent signals. It can be extended to multicomponent nonstationary signals by using signal decomposition methods such as T-F blind source separation [9] or by designing data dependent reduced interferences TFDs for the multicomponent signals case [11]. Further work could also focus on exploring other possible forms of lower order CTDs with less bias and variance of the IF estimate to maximize the estimation accuracy while preserving robustness to noise.

5. Conclusion

This paper presents a robust method for estimating highly-changing nonlinear IFs in monocomponent signals using a lower order CTD based on the general concept of complex-time argument differentiation [18]. The proposed IF estimation approach retains the high tracking ability of the IF law with robustness to noise while avoiding issues related to the interference terms. The performance of the approach was

evaluated and compared with the classical WVD as well as the L-form CTDs which are capable of dealing with highly nonstationary signals [19,26]. In high levels of noise (SNR of -10 to 5 dB), the proposed lower-order CTD (used in conjunction with the peak frequency detector) generates the lowest NRMSE cost amongst the other methods compared in this study. For higher SNRs (5 to 20 dB) and highly-changing nonlinear IFs, the lower-order CTD also outperforms the others. However, the bias and variance of the proposed method is higher than the 4th and 6th order LCTDs in the absence of noise. The findings suggest that avoiding high order derivatives in IF estimation methods improves their robustness to noise. The proposed method can be extended to multicomponent nonstationary signals by using nonstationary signal decomposition approaches such as time–frequency blind source separation [9] and reduced interferences realization [11], with the potential of allowing more advanced applications of time–frequency signal analysis in various fields of science, engineering and medicine.

Acknowledgments

This publication was supported by a grant from the Qatar National Research Fund under its National Priorities Research Program award number NPRP 09-465-2-174.

Appendix. Key steps for the new TFD properties proofs

P1. Realness: $W_z^{CL}(t, f)$ is always real for signals with the general form described in Eq. (1).

Proof. Let us consider the case where the function $\varphi(t)$ is differentiable or more generally, $\varphi(z)$ is holomorphic (analytic). From the basic properties of holomorphic functions, we have:

$$\begin{aligned} \varphi(z)^* &= \varphi(z^*) \\ \Rightarrow \text{Re}\{\varphi(t + j\tau)\} - j\text{Im}\{\varphi(t + j\tau)\} &= \text{Re}\{\varphi(t - j\tau)\} + j\text{Im}\{\varphi(t - j\tau)\}. \end{aligned} \quad (35)$$

and:

$$\text{Im}\{\varphi(t - j\tau)\} = -\text{Im}\{\varphi(t + j\tau)\} \quad (36)$$

The complex conjugate of $W_z^{CL}(t, f)$ is then written as

$$W_z^{CL*}(t, f) = \int_{-\infty}^{\infty} e^{-j\text{Im}\{\varphi(t+j\tau)\}} e^{j2\pi f\tau} d\tau. \quad (37)$$

A change of variable from τ to $-\tau$ leads to

$$\begin{aligned} W_z^{CL*}(t, f) &= - \int_{\infty}^{-\infty} e^{-j\text{Im}\{\varphi(t-j\tau)\}} e^{-j2\pi f\tau} d\tau = \int_{-\infty}^{\infty} e^{j\text{Im}\{\varphi(t+j\tau)\}} e^{-j2\pi f\tau} d\tau \\ &= W_z^{CL}(t, f). \end{aligned} \quad (38)$$

Therefore, the unsmoothed $\rho_z^{CL}(t, f)$ is real.

P2. Time shift: if $W_z^{CL}(t, f)$ is the unsmoothed distribution of signal $z(t)$, then $W_z^{CL}(t - T, f)$ is the unsmoothed distribution of signal $z(t - T)$.

Proof. Let $W_z^{CL}(t, f)$ be a TFD of the signal $z(t)$ with the signal kernel $K_z^{CL}(t, \tau)$. The TFD with a shift in time can be written as

$$W_z^{CL}(t-T, f) = \int_{-\infty}^{\infty} K_z^{CL}(t-T, \tau) e^{-j2\pi f \tau} d\tau = \int_{-\infty}^{\infty} e^{jlm\{\varphi(t-T+j\tau)\}} e^{-j2\pi f \tau} d\tau. \quad (39)$$

On the other hand, considering Eqs. (14) and (1), it follows that $K_z^{CL}(t-T, \tau)$ is the signal kernel of the signal $z(t-T)$.

P3. Frequency shift: if $W_z^{CL}(t, f)$ is the unsmoothed TFD of a signal $z(t)$, then $W_z^{CL}(t, f-f_0)$ is the unsmoothed distribution of the signal $z(t)e^{j2\pi f_0 t}$.

Proof

$$z_2(t) = z(t)e^{j2\pi f_0 t} = e^{j(\varphi(t)+2\pi f_0 t)} = e^{j\varphi_2(t)} \\ \Rightarrow \varphi_2(t+j\tau) = \varphi(t+j\tau) + 2\pi f_0 t + j2\pi f_0 \tau. \quad (40)$$

$K_{z_2}^{CL}(t, \tau)$ is then written as

$$K_{z_2}^{CL}(t, \tau) = e^{jlm\{\varphi_2(t+j\tau)\}} = e^{jlm\{\varphi(t+j\tau)\}} e^{j2\pi f_0 \tau}. \quad (41)$$

$W_{z_2}^{CL}(t, f)$ is obtained by taking the Fourier transform of $K_{z_2}^{CL}(t, \tau)$:

$$W_{z_2}^{CL}(t, f) = \int_{-\infty}^{\infty} K_{z_2}^{CL}(t, \tau) e^{-j2\pi f \tau} d\tau \\ = \int_{-\infty}^{\infty} e^{jlm\{\varphi(t+j\tau)\}} e^{j2\pi f_0 \tau} e^{-j2\pi f \tau} d\tau = W_z^{CL}(t, f-f_0). \quad (42)$$

P4. Time-frequency scaling: if $W_z^{CL}(t, f)$ is the TFD of $z(t)$, then the TFD of the scaled signal $z(at)$ is $1/|a|W_z^{CL}(at, f/a)$.

Proof:

$$z_2(t) = z(at) = e^{j\varphi(at)} \Rightarrow z_2(a(t+j\tau)) = e^{j\varphi(a(t+j\tau))} \quad (43)$$

The signal kernel is written as

$$K_{z_2}^{CL}(t, \tau) = e^{jlm\{\varphi(a(t+j\tau))\}} \\ \Rightarrow W_{z_2}^{CL}(t, f) = \int_{-\infty}^{\infty} K_{z_2}^{CL}(t, \tau) e^{-j2\pi f \tau} d\tau \\ = \int_{-\infty}^{\infty} e^{jlm\{\varphi(a(t+j\tau))\}} e^{-j2\pi f \tau} d\tau. \quad (44)$$

By changing variable $\tau' = a\tau$ and substituting into Eq. (44), we have:

$$ad\tau = d\tau' \Rightarrow W_{z_2}^{CL}(t, f) = \frac{1}{|a|} \int_{-\infty}^{\infty} e^{jlm\{\varphi(a(t+j\tau'))\}} e^{-j2\pi(f/a)\tau'} d\tau' \\ = \frac{1}{|a|} W_z^{CL}(at, f/a). \quad (45)$$

P5. Time marginal: integration of $W_z^{CL}(t, f)$ over the frequency axis (time marginal distribution) results in Eq. (25).

Proof. Using the DC offset property of the Fourier transform for signals with the general form of Eq. (1), Eq. (25) can be re-written as [16]

$$\int_{-\infty}^{\infty} W_z^{CL}(t, f) df = K_z^{CL}(t, \tau)|_{\tau=0}. \quad (46)$$

Combining the right side of Eq. (46) and (15) leads directly to Eq. (25).

P6. Instantaneous frequency: the first order moment of $W_z^{CL}(t, f)$ with respect to frequency yields the IF of the signal $z(t)$.

Proof. The first order moment (i.e. the mean) of $W_z^{CL}(t, f)$ with respect to frequency is defined as [1]

$$\langle f \rangle_t \triangleq \frac{\int_{-\infty}^{\infty} f W_z^{CL}(t, f) df}{\int_{-\infty}^{\infty} W_z^{CL}(t, f) df}. \quad (47)$$

Using the DC offset and differentiation properties of the Fourier transform, Eq. (47) can be expressed as [16]

$$\langle f \rangle_t = \frac{\frac{1}{2\pi j} \frac{\partial K_z^{CL}(t, \tau)}{\partial \tau} |_{\tau=0}}{K_z^{CL}(t, \tau)|_{\tau=0}}. \quad (48)$$

From Eq. (15), the derivative of $K_z^{CL}(t, \tau)$ with respect to τ in Eq. (48) is given by

$$\frac{\partial K_z^{CL}(t, \tau)}{\partial \tau} = j \frac{\partial lm\{\varphi(t+j\tau)\}}{\partial \tau} e^{jlm\{\varphi(t+j\tau)\}}. \quad (49)$$

Combining Eqs. (12) and (49) results in:

$$\frac{\partial lm\{\varphi(t+j\tau)\}}{\partial \tau} = \varphi'(t) - \frac{\tau^2}{2!} \varphi'''(t) + \dots \quad (50)$$

Combining Eqs. (48)–(50) leads to $\langle f \rangle_t$ in Eq. (48) which in turn, results in the instantaneous frequency of $W_z^{CL}(t, f)$ at time t (Eq. (26)).

P7. Modulation invariance: if $z(t) = z_1(t)z_2(t)$ and $z_1(t)$ and $z_2(t)$ are of the form of Eq. (1) then $W_z^{CL}(t, f)$ is obtained by Eq. (27).

Proof. Suppose $z_1(t) = e^{j\varphi_1(t)}$ and $z_2(t) = e^{j\varphi_2(t)}$. The IAF $K_z^{CL}(t, \tau)$ is then given by

$$K_z^{CL}(t, \tau) = |z(t+j\tau)|^{-j} = |z_1(t+j\tau)|^{-j} |z_2(t+j\tau)|^{-j} = K_{z_1}(t, \tau) K_{z_2}(t, \tau). \quad (51)$$

Taking the inverse Fourier transform of Eq. (51) with respect to τ leads to Eq. (27).

References

- [1] B. Boashash, Time-Frequency Signal Analysis and Processing: A Comprehensive Reference, Elsevier, Amsterdam; Boston, 2003.
- [2] I. Orović, S. Stanković, T. Thayaparan, L.J. Stanković, Multiwindow S-method for instantaneous frequency estimation and its application in radar signal analysis, IET Signal Processing 4 (2010) 363–370.
- [3] B. Boashash, P. O'Shea, A methodology for detection and classification of some underwater acoustic signals using time-frequency analysis techniques, IEEE Transactions on Acoustics, Speech and Signal Processing 38 (1990) 1829–1841.
- [4] G. Azemi, B. Senadji, B. Boashash, Mobile unit velocity estimation based on the instantaneous frequency of the received signal, IEEE Transactions on Vehicular Technology 53 (2004) 716–724.
- [5] B. Boashash, Estimating and interpreting the instantaneous frequency of a signal. I. Fundamentals, Proceedings of the IEEE 80 (1992) 520–538.

- [6] B. Boashash, Estimating and interpreting the instantaneous frequency of a signal. II. Algorithms and applications, *Proceedings of the IEEE* 80 (1992) 540–568.
- [7] V. Susic, N. Saulig, B. Boashash, Estimating the number of components of a multicomponent nonstationary signal using the short-term time–frequency Renyi entropy, *EURASIP Journal of Advances in Signal Processing* 2011 (2011) 125.
- [8] D. Rudrauf, A. Douiri, C. Kovach, J.P. Lachaux, D. Cosmelli, M. Chavez, C. Adam, B. Renault, J. Martinerie, M. Le Van Quyen, Frequency flows and the time–frequency dynamics of multivariate phase synchronization in brain signals, *NeuroImage* 31 (2006) 209–227.
- [9] B. Barkat, K. Abed-Meraim, A blind components separation procedure for FM signal analysis, in: *Proceedings of the IEEE International Conference on Acoustics, Speech, and Signal Processing*, 2002, pp. II-1425–II-1428.
- [10] J. Lerga, V. Susic, B. Boashash, An efficient algorithm for instantaneous frequency estimation of nonstationary multicomponent signals in low SNR, *EURASIP Journal on Advances in Signal Processing* 2011 (2011) 725189.
- [11] L. Stankovic, Time–frequency distributions with complex argument, *IEEE Transactions on Signal Processing* 50 (2002) 475–486.
- [12] P.M. Djuric, S.M. Kay, Parameter estimation of chirp signals, *IEEE Transactions on Acoustics, Speech and Signal Processing* 38 (1990) 2118–2126.
- [13] S. Peleg, B. Porat, Estimation and classification of polynomial-phase signals, *IEEE Transactions on Information Theory* 37 (1991) 422–430.
- [14] L. Stanković, A multitime definition of the Wigner higher order distribution: L-Wigner distribution, *Signal Processing Letters, IEEE* 1 (1994) 106–109.
- [15] B. Barkat, B. Boashash, Design of higher order polynomial Wigner–Ville distributions, *IEEE Transactions on Signal Processing* 47 (1999) 2608–2611.
- [16] B. Boashash, B. Ristic, Polynomial time–frequency distributions and time-varying higher order spectra: application to the analysis of multicomponent FM signals and to the treatment of multiplicative noise, *Signal Processing* 67 (1998) 1–23.
- [17] S. Stanković, N. Zarić, C. Ioana, General form of time–frequency distribution with complex-lag argument, *Electronics Letters, IEEE* 44 (2008) 699–701.
- [18] S. Stanković, L. Stanković, Introducing time–frequency distribution with a 'complex-time' argument, *Electronics Letters, IEEE* 32 (1996) 1265–1267.
- [19] I. Orović, M. Orlandić, S. Stanković, Z. Uskoković, A virtual instrument for time–frequency analysis of signals with highly nonstationary instantaneous frequency, *IEEE Transactions on Instrumentation and Measurement* 60 (2011) 791–803.
- [20] I. Orovic, A. Draganic, S. Stankovic, E. Sejdic, A unified approach for the estimation of instantaneous frequency and its derivatives for non-stationary signals analysis, in: *Proceedings of the IEEE 11th International Conference on Information Science, Signal Processing and their Applications*, Montreal, Canada, 2012.
- [21] N. Zaric, I. Orovic, S. Stankovic, Robust time–frequency distributions with complex-lag argument, *EURASIP Journal of Advances in Signal Processing* 2010 (2010) 1–10.
- [22] W. Squire, G. Trapp, Using complex variables to estimate derivatives of real functions, *SIAM Review* 40 (1998) 110–112.
- [23] K.L. Lai, J.L. Crassidis, Extensions of the first and second complex-step derivative approximations, *Journal of Computational and Applied Mathematics* 219 (2008) 276–293.
- [24] J. Martins, P. Sturda, J. Alonso, The complex-step derivative approximation, *ACM Transactions on Mathematical Software* 29 (2003) 245–262.
- [25] B. Boashash, P. O'Shea, Polynomial Wigner–Ville distributions and their relationship to time-varying higher order spectra, *IEEE Transactions on Signal Processing* 42 (1994) 216–220.
- [26] S. Stankovic, I. Orovic, C. Ioana, Effects of cauchy integral formula discretization on the precision of IF estimation: unified approach to complex-lag distribution and its counterpart L-form, *Signal Processing Letters, IEEE* 16 (2009) 327–330.
- [27] M.S. Ridout, Statistical applications of the complex-step method of numerical differentiation, *The American Statistician* 63 (2009) 66–74.
- [28] M. Morelande, B. Senadji, B. Boashash, Complex-lag polynomial Wigner–Ville distribution, in: *Proceedings of the IEEE Annual Conference on Speech and Image Technologies for Computing and Telecommunications*, vol. 1, 1997, pp. 43–46.
- [29] B. Boashash, T. Ben-Jabeur, Design of a high-resolution separable-kernel quadratic TFD for improving newborn health outcomes using fetal movement detection, in: *Proceedings of the IEEE 11th International Conference on Information Science, Signal Processing and their Applications*, 2012, pp. 354–359.
- [30] B. Boashash, Efficient software implementation for the upgrade of a time–frequency signal analysis package, in: *Proceedings of the 8th Australian Joint Conference on Artificial Intelligence and Applications* Canberra, Australia, 1995, pp. 26–31, available from: <http://www.time-frequency.net>.